SU(2) Lattice Gauge Theory: Standard Action Versus Symanzik's Tree-Improved Action

B. Berg[1], A. Billoire[2], S. Meyer[3]⋆, and C. Panagiotakopoulos[4]

1 II. Institut für Theoretische Physik der Universität Hamburg, Luruper Chaussee 149,
D-2000 Hamburg 50, Federal Republic of Germany
2 CEN Saclay, Service de Physique Théorique, Orme des Merisiers, F-91191 Gif-sur-Yvette
Cedex, France
3 Fachbereich Physik der Universität Kaiserslautern, Erwin-Schrödinger-Strasse,
D-6750 Kaiserslautern, Federal Republic of Germany
4 Physics Department (Theory), The Rockefeller University, 1230 York Avenue, New York,
NY 10021-6399, USA

Dedicated to the memory of Kurt Symanzik

Abstract. We carry out Monte Carlo simulations of the $4d$ SU(2) lattice gauge theory. The standard action and the Symanzik tree-improved action are used. Results for the string tension, glueball masses, and energy-momentum dispersion are reported. In case of the standard action our results are a finite size study extending previous investigations.

I. Introduction

Symanzik [1, 2] has pointed out that corrections to continuum theory stemming from finite lattice spacing can be systematically diminished by use of a judiciously chosen lattice action. A number of Monte Carlo (MC) studies [3] have been carried out using Symanzik improved action. In this paper we report high statistics results for $4d$ SU(2) lattice gauge theory.

In the continuum limit each physical quantity is proportional to an appropriate power of the correlation length (inverse mass gap) ξ with an universal coefficient. For non-zero lattice spacing $a \neq 0$ this "scaling" is violated by non-universal terms of order $(a^2/\xi^2)\ln(a/\xi)$. Symanzik improved actions allow us to reduce these violations to order $(a^2/\xi^2)^2\ln(a/\xi)$, to all orders of perturbation theory, by including in the lattice action suitable chosen irrelevant terms.

In principle the coefficients of these irrelevant terms can be calculated up to any given order of perturbation theory. For $4d$ SU(n) lattice gauge theories the tree-level improved action (TIA) has been determined [4–6]. A motivated ansatz [5] for the improved action includes Wilson loops up to length 6 and the result

---

[4, 6] for the TIA becomes

$$S^{TI} = -\frac{4}{g^2}\left[\frac{5}{3}\sum_{\square}\text{Re}(\text{Tr}\,\square) - \frac{1}{12}\sum_{\square\square}\text{Re}(\text{Tr}\,\square\square)\right]. \tag{I.1}$$

Here $\square\square$ represents the planar rectangular double plaquettes of size 1×2.

We carry out a high statistics MC simulation using
a) the standard action (SA) on an 8^4 lattice,
b) the TIA on $5^3 \cdot 8$ and 8^4 lattices.

We are mainly interested in calculating the glueball mass spectrum[1] for both actions. We use a variant of the MC variational (MCV) method, which was pioneered in [8–10]. The Wilson loops involved in our calculations are numerated in Fig. I.1. Following the classification of [11] we construct states in various irreducible representations of the cubic group. For more details about the glueball calculations see Sect. II.2.
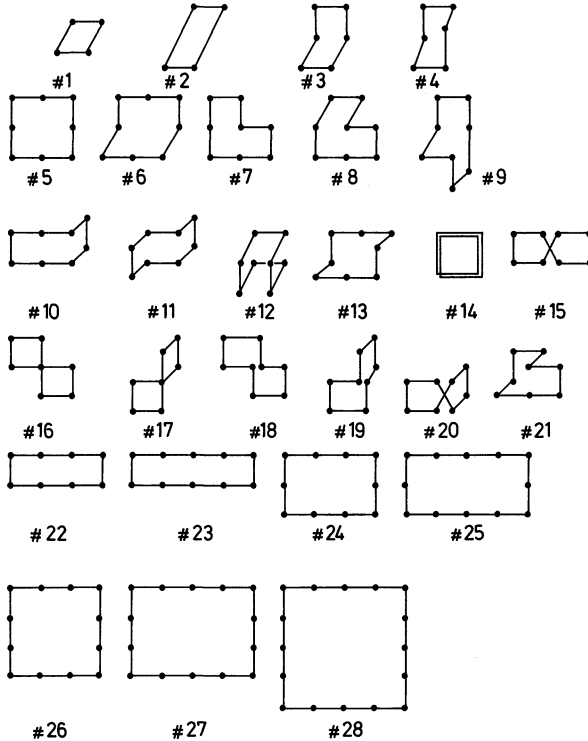

Fig. I.1. Wilson loops as used in this paper

For some operators we also calculate the energies of momentum eigenstates and consider the relativistic energy-momentum dispersion. In the $2d$ O(3) non-linear σ-model such an analysis was previously carried out in [12]. Improvement was found for the 1-loop improved action, but not for the TIA. In the present case the TIA behaves even worse than the SA.

---

1   For a recent review of glueball calculations in lattice gauge theories, see [7]

In case of the SA a scaling window for the 0^+ glueball (mass gap) was first obtained in [8]. The MCV method was used on a $4^3 \cdot 16$ lattice, leading to the estimate

$$m(0^+) = (170 \pm 30)\Lambda_L. \tag{I.2}$$

In this paper we present a finite size study of this and other results [10] obtained on small lattices. Previous [13, 14] investigations on an 8^4 lattice are improved and corrected. Our *final* $m(0^+)$ estimate is well consistent with the estimate (I.2).

As a byproduct we obtain high statistics data for Creutz [15] ratios up to $\chi(4,4)$. This allows an improvement of previous string tension estimates (for instance [15, 16]) which were mainly based on $\chi(3,3)$. Creutz ratios $\chi(I,J)$ are not stable under increasing (I,J) from $(3,3)$ to $(4,4)$, and the string tension has a decreasing tendency. The potential analysis of [17] on a 15^4 lattice and measurements of Polyakov loop correlation functions [18, 19] indicate that this process continues also beyond the estimate one obtains from $\chi(4,4)$.

In the case of the TIA we have assembled very large statistics on a $5^3 \cdot 8$ lattice, on which our glueball estimates are based. This improves previously reported results [20]. It has to be emphasized [21] that the TIA has severe problems with the transfer matrix. The transfer matrix is not positive definite, not even symmetric. It connects three time-layers. Therefore, the MCV method has problems, and the smallest distance, where we can expect to get meaningful results is $t = 2$.

As in [12] we distinguish in this paper scaling in the general sense and asymptotic scaling. Scaling in general means scaling with respect to the (unknown) lattice β-function, and asymptotic scaling means scaling with respect to the *universal* part of the β-function. Asymptotic scaling implies proportionality of a physical quantity with respect to a standard two-loop Λ_L scale. The improvement program [1, 2, 4–6] is made for general scaling. Interesting quantities are mass ratios for which we have

$$\frac{m_1}{m_2} \simeq \left(\frac{a^2}{\xi_r^2}\right)\ln\left(\frac{a}{\xi_r}\right) \rightarrow \left(\frac{a^2}{\xi_r^2}\right)^2 \ln\left(\frac{a}{\xi_r}\right) \tag{I.3}$$

up to the considered order of the coupling g^2. In Eq. (I.3) we have introduced the "relevant range of interaction" [7] $\xi_r = \alpha\xi$. The parameter α should be adjusted, such that the proportionality constant in (I.3) is numerically close to 1. Typically $\alpha \approx 4$ for $4d$ lattice gauge theories. This emphasizes the meaning of the correlation length ξ as a counting parameter for (a^2/ξ^2) corrections to scaling and indicates that improvement may already work at a correlation length $\xi < 1$.

The string tension for the SU(2) TIA was first studied in [22, 23]. The MC statistics of these investigations, particularly of [22], is rather poor. Therefore, we did a calculation with a more reasonable MC statistics on an 8^4 lattice. We obtain results for Creutz ratios up to $\chi(4,4)$. Also improved Creutz ratios [6] are studied and found to converge better with respect to the loop size. This indicates nicely that improvement is sensible in the considered $\beta = 4/g^2$-region. However, the potential analysis [17] indicates again a further lowering of the string tension beyond the result as obtained from $\chi(4,4)$.

Our paper is organized as follows: Section II contains our SA results, Sect. III the TIA results, and finally, summary and conclusions are presented in Sect. IV.

Table II.1. Rectangular Wilson loops

β	2.20	2.25	2.30	2.35	2.40	2.50
Sweeps (Eq)	40,000 (1,200)	60,000 (1,200)	60,000 (1,200)	60,000 (1,200)	60,000 (1,200)	60,000 (1,200)
Measurements (Bins)	20,000 (20)	24,000 (20)	24,000 (20)	20,000 (16)	20,000 (20)	20,000 (20)
W_{11}	0.56928 ±0.00008	0.58619 ±0.00008	0.60215 ±0.00008	0.61690 ±0.00011	0.63025 ±0.00008	0.65241 ±0.00005
W_{12}	0.34126 ±0.00012	0.36385 ±0.00012	0.38575 ±0.00013	0.40646 ±0.00017	0.42551 ±0.00014	0.45733 ±0.00008
W_{22}	0.13644 ±0.00013	0.15767 ±0.00014	0.17976 ±0.00017	0.20186 ±0.00022	0.22315 ±0.00021	0.25971 ±0.00014
W_{13}	0.20682 ±0.00013	0.22862 ±0.00012	0.25049 ±0.00014	0.27173 ±0.00019	0.29178 ±0.00016	0.32594 ±0.00010
W_{14}	0.12562 ±0.00012	0.14403 ±0.00011	0.23071 ±0.00013	0.18228 ±0.00018	0.20082 ±0.00016	0.23325 ±0.00011
W_{23}	0.05716 ±0.00011	0.07192 ±0.00010	0.08848 ±0.00015	0.10626 ±0.00020	0.12436 ±0.00020	0.15706 ±0.00016
W_{24}	0.02426 ±0.00007	0.03330 ±0.00007	0.04424 ±0.00011	0.05691 ±0.00015	0.07057 ±0.00017	0.09683 ±0.00015
W_{33}	0.01747 ±0.00008	0.02518 ±0.00007	0.03505 ±0.00011	0.04683 ±0.00010	0.05992 ±0.00018	0.08566 ±0.00018
W_{34}	0.00554 ±0.00005	0.00915 ±0.00005	0.01437 ±0.00008	0.02140 ±0.00010	0.03003 ±0.00013	0.04867 ±0.00015
W_{44}	0.00137 ±0.00005	0.00271 ±0.00003	0.00501 ±0.00005	0.00855 ±0.00008	0.01363 ±0.00011	0.02613 ±0.00015

II. The Standard Action

In this section we report our MC results as obtained with the SA. We use the icosaeder SU(2) subgroup [24], our simulation is carried out on an 8^4 lattice. Our main interest is concerned with the glueball spectrum. Therefore, we concentrate on a few important β-values and collect at each β-value very high statistics, as is obvious from Table II.1. As in [11] we use random upgrading and a sweep is defined by upgrading each link once in the mean. After two sweeps ($\beta \leq 2.30$), three sweeps ($\beta \geq 2.35$) measurements are performed. As analyzed in [11] this is expected to save computer time as compared with calculating up to a similar accuracy by doing measurements after each sweep. We have used the Metropolis method with 5 trials per upgrading. A typical acceptance rate for 5 trials is 70%.

For each measurement we select a time direction (which is cyclically rotated for the next measurement etc.) and calculate in each $t = $ const plane the vacuum expectation values for all Wilson loops up to length 8 and additionally for the rectangular loops up to size $4 \cdot 4$. The Wilson loops are numerated in Fig. I.1. Our

Table II.2. Creutz ratios

β	2.20	2.25	2.30	2.35	2.40	2.50
$\chi(1,1)$	0.5634	0.5341	0.5072	0.4830	0.4616	0.42708
	± 0.0002	± 0.0002	± 0.0002	± 0.0002	± 0.0002	± 0.00007
$\chi(1,2)$	0.5117	0.4769	0.4453	0.4172	0.3928	0.35526
	± 0.0003	± 0.0002	± 0.4453	± 0.0003	± 0.0002	± 0.00011
$\chi(2,2)$	0.4051	0.3594	0.3181	0.2827	0.2526	0.21058
	± 0.0005	± 0.0004	± 0.0004	± 0.0005	± 0.0005	± 0.00027
$\chi(1,3)$	0.5008	0.4646	0.4317	0.4027	0.3773	0.33871
	± 0.0003	± 0.0002	± 0.0003	± 0.0003	± 0.0003	± 0.00014
$\chi(1,4)$	0.4986	0.4620	0.4287	0.3993	0.3736	0.33460
	± 0.0004	± 0.0002	± 0.0003	± 0.0003	± 0.0003	± 0.00016
$\chi(2,3)$	0.3693	0.3205	0.2769	0.2390	0.2074	0.1643
	± 0.0007	± 0.0004	± 0.0005	± 0.0006	± 0.0005	± 0.0004
$\chi(2,4)$	0.3583	0.3084	0.2640	0.2251	0.1929	0.1491
	± 0.0011	± 0.0006	± 0.0006	± 0.0007	± 0.0007	± 0.0005
$\chi(3,3)$	0.3154	0.2649	0.2169	0.1778	0.1456	0.1032
	± 0.0023	± 0.0011	± 0.0008	± 0.0007	± 0.0009	± 0.0007
$\chi(3,4)$	0.2910	0.2421	0.1979	0.1586	0.1242	0.0818
	± 0.0044	± 0.0018	± 0.0015	± 0.0011	± 0.0011	± 0.0007
$\chi(4,4)$	0.251	0.2115	0.1657	0.1350	0.0992	0.0563
	± 0.029	± 0.0081	± 0.0046	± 0.0042	± 0.0028	± 0.0015

notation for expectation values of rectangular loops of size $I \cdot J$ is W_{IJ} and our normalization is $\lim_{\beta \to \infty} W_{IJ}(\beta) = 1$. We obtain high precision expectation values for these loops. The results for rectangular loops are collected in Table II.2. In most of the cases the statistical analysis is done with respect to 20 bins considered as typical "independent events". This means that a typical "independent event" is an average over 1000 measurements done over 2000–3000 sweeps.

At $\beta = 2.2$, 2.3, 2.4, and 2.5 some values can be compared with those of [16], where the full SU(2) group and the heat bath method was used. Within statistical errors (Table 5 of [16], where all Wilson loops (including timelike directions) were measured after each sweep (systematic upgrading), has to be used) we find agreement up to $\beta = 2.4$. At $\beta = 2.5$ a small systematic lowering is observed. Using the measured Wilson loops we obtain high statistics results for the string tension relying in Creutz ratios. These results are presented in Sect. II.1.

For each measured Wilson loop (in each $t = $ const plane) we construct various irreducible representations of the cubic group (see [11] for details) and keep on-diagonal correlations up to distance $t = 2$ for excited states and up to distance $t = 3$ for the 0^+ state. For some operators we also calculate momentum $\mathbf{p} \neq 0$ eigenstates (see Sect. II.5). Our spectrum results are presented in Sects. II.2–II.4: The $m(0^+)$ mass gap in Sect. II.2, excited glueball states in Sect. II.3 and finally the energy-momentum dispersion is studied in Sect. II.4.
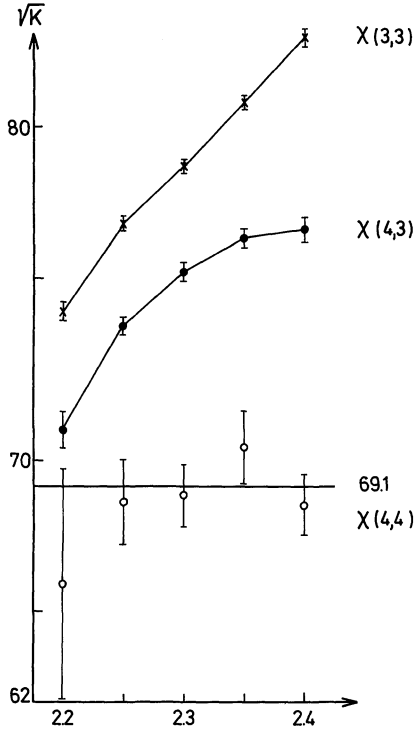
Fig. II.1. String tension estimate (in units of Λ_L^{SA}) from Creutz ratios

II.1. The String Tension

From our measured rectangular Wilson loops (Table II.1) we obtain high precision results for the Creutz [15] ratios

$$\chi(I, J) = -\ln\left(\frac{W_{IJ} \cdot W_{I-1, J-1}}{W_{I-1, J} \cdot W_{I, J-1}}\right) \tag{II.1}$$

up to $I = J = 4$. These results are listed in Table II.2. Previous MC investigations (for instance [15, 16]) had only a sufficient statistics for obtaining reliable results up to $\chi(3, 3)$ and led to continuum estimates of the string tension of order

$$\sqrt{K} \approx 76 \, \Lambda_L^{SA}. \tag{II.2}$$

We have now a nearly 100 times larger statistics than in [16]. The new very precise data for $\chi(3, 3)$ are within statistical errors consistent with the early data. In Fig. II.1 we plot our present results for $\chi(3, 3)$, $\chi(4, 3)$, and $\chi(4, 4)$ in physical units of Λ_L. On the detailed scale of this figure we realize clear deviations from asymptotic scaling for $\chi(3, 3)$. The situation is improving for $\chi(4, 3)$ and $\chi(4, 4)$. Within statistical errors the $\chi(4, 4)$ data are consistent with asymptotic scaling and lead to the continuum estimate

$$\sqrt{K} \approx 69 \, \Lambda_L^{SA}. \tag{II.3}$$

There are, however, evidences that the string tension is in fact lower. The first one comes from a measurement of Wilson loops on a 15^4 lattice [17]. Fitting the potential to a Coulomb plus linear form, results in a considerable lowering of the string tension estimate. The final $\sqrt{K}$ estimate is

$$\sqrt{K} \approx 56\, \Lambda_L^{SA}. \qquad (II.4)$$

As asymptotic scaling deviations are also reported, the meaning of this number for the continuum limit is, however, obscure. Further, clarification is desirable.

The second evidence that the string tension is in fact lower than II.3 comes from investigations of Polyakov loop correlations [18]. As a Polyakov loop wraps around the whole lattice, this method gives a better estimate of the quark anti-quark potential. After projection on zero momentum, the estimate of the string tension becomes very stable with respect to the distance between the two loops. Results are consistent with asymptotic scaling leading to the estimate

$$\sqrt{K} \approx 52\, \Lambda_L^{SA}.$$

Comparing our $\chi(4,4)$ results with those of [17] (on a 15^4 lattice) we find agreement except for $\beta = 2.4$, where finite lattice effects may well be important for a 4×4 loop (our lattice is 8^4). For the other β-values finite size effects on $\chi(4,4)$ are small. Therefore, our scaling for $\chi(4,4)$ might be a finite size effect.

II.2. The Mass Gap $m(0^+)$

The aim of this section is to investigate the previous MCV mass gap estimate [8] [2] relying on calculations on a $4^3 \cdot 16$ lattice, with respect to finite lattice size effects. Further, the use of a larger lattice will allow us to extend the scaling window beyond $\beta = 2.25$ up to $\beta = 2.4$. We project our 28 Wilson loops into the A_1^+ representation and measure on-diagonal correlations up to distance $t = 3$. For each of these operators we define distance t glueball masses by means of

$$m_i(t_2, t_1) = \frac{-1}{t_2 - t_1} \ln\left(\frac{\langle 0_i(0)0_i(t_2)\rangle}{\langle 0_i(0)0_i(t_1)\rangle}\right) \qquad (t_2 > t_1). \qquad (II.5)$$

In the infinite statistics limit all these numbers become upper bounds for the real mass gap $m(0^+)$. Due to technical reasons (disk space and tape handling) we did not measure off-diagonal correlations and therefore minimization in the sense of [8–10] is not possible. In the spirit of minimization we take our final estimates from the single operators, which give the lowest results for $m_i(1,0)$ $(i = 1, ..., 28)$. By definition these operators are called the "*best*" operators. In view of our experience [8, 11] that at distance $t = 2$, for good operators, statistical noise is already overwhelming the effect of minimization, we expect rather reliable results. To take directly the smallest value $m(2,1)$ $(i = 1, ..., 28)$ is not correct, because we would obtain a too small result due to statistical fluctuations. In fact, the pattern of operators which give low results at distance $t = 2$ is rather unstable with respect to β, whereas it is stable at distance $t = 1$.

---

2   Similar estimates were obtained by other authors. For a review see [7]

Table II.3. $m(0^+)$ results from the best three operators

β	OP	$m(1, 0)$	$m(2, 0)$	$m(2, 1)$
2.20	6	1.79 ± 0.03	1.75 ± 0.07	1.72 ± 0.14
2.20	13	1.78 ± 0.03	1.73 ± 0.07	1.68 ± 0.14
2.20	21	1.79 ± 0.03	1.73 ± 0.06	1.67 ± 0.14
2.25	6	1.69 ± 0.02	1.53 ± 0.03	1.37 ± 0.07
2.25	13	1.68 ± 0.02	1.54 ± 0.03	1.40 ± 0.08
2.25	21	1.71 ± 0.02	1.56 ± 0.03	1.47 ± 0.08
2.30	6	1.64 ± 0.03	1.42 ± 0.03	1.20 ± 0.08
2.30	13	1.63 ± 0.03	1.41 ± 0.03	1.20 ± 0.09
2.30	21	1.65 ± 0.03	1.42 ± 0.03	1.19 ± 0.09
2.35	6	1.73 ± 0.03	1.55 ± 0.04	1.36 ± 0.09
2.35	13	1.72 ± 0.03	1.54 ± 0.04	1.36 ± 0.09
2.35.	21	1.78 ± 0.03	1.60 ± 0.04	1.42 ± 0.10
2.40	6	1.80 ± 0.03	1.52 ± 0.04	1.23 ± 0.09
2.40	13	1.78 ± 0.03	1.50 ± 0.04	1.21 ± 0.09
2.40	24	1.78 ± 0.03	1.44 ± 0.04	1.11 ± 0.09
2.50	24	2.03 ± 0.03	1.64 ± 0.05	1.25 ± 0.11
2.50	25	2.06 ± 0.04	1.62 ± 0.04	1.18 ± 0.10
2.50	27	2.11 ± 0.04	1.59 ± 0.04	1.08 ± 0.10

In Table II.3 we have collected for the three best operators the results up to distance $t = 2$. For all three operators the $m(2, 1)$ results are always identical within statistical errors. Only for $\beta \geq 2.4$ operators with length > 8 are among the best operators.

Previously a finite size study, also on an 8^4 lattice, was attempted by Ishikawa et al. [13, 14]. Unfortunately, these authors used "momentum smeared" wave functions to improve the MC statistics, then the unknown $\mathbf{p}^2$-contribution was subtracted by introducing one new parameter. In Fig. II.2 we compare their results
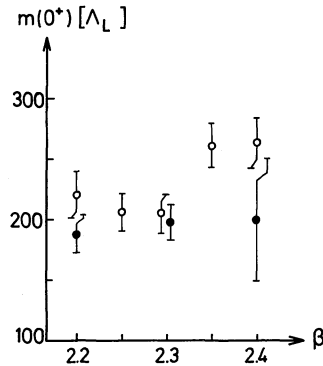

Fig. II.2. Our momentum $\mathbf{p} = 0$ results (φ) in comparison with results ($\bullet$) from [13, 14] as obtained from "momentum smeared" wave functions

Table II.4. $m(0^+)$ distance $t = 3$ results from the best three operators

β	OP	$m(3, 0)$	$m(3, 1)$	$m(3, 2)$
2.20	6	$1.84 \pm^{1.03}_{0.20}$	$1.87 \pm^{1.55}_{0.35}$	$2.01 \pm^{3.20}_{0.79}$
2.20	13	$1.85 \pm^{0.77}_{0.22}$	$1.88 \pm^{1.17}_{0.33}$	$2.08 \pm^{2.43}_{0.78}$
2.20	21	$1.94 \pm^{\infty}_{0.30}$	$2.01 \pm^{\infty}_{0.39}$	$2.35 \pm^{\infty}_{0.88}$
2.25	6	1.41 ± 0.07	$1.27 \pm^{0.11}_{0.09}$	$1.17 \pm^{0.24}_{0.21}$
2.25	13	1.41 ± 0.07	1.27 ± 0.10	$1.14 \pm^{0.24}_{0.22}$
2.25	21	1.42 ± 0.07	1.28 ± 0.10	$1.15 \pm^{0.25}_{0.23}$
2.35	6	1.37 ± 0.08	1.18 ± 0.12	$0.96 \pm^{0.29}_{0.25}$
2.35	13	$1.39 \pm^{0.10}_{0.07}$	$1.22 \pm^{0.16}_{0.12}$	$1.04 \pm^{0.34}_{0.29}$
2.35	21	$1.45 \pm^{0.10}_{0.07}$	$1.28 \pm^{0.17}_{0.13}$	$1.10 \pm^{0.37}_{0.31}$
2.40	6	1.27 ± 0.05	1.00 ± 0.09	0.78 ± 0.22
2.40	13	1.25 ± 0.05	0.98 ± 0.08	0.76 ± 0.20
2.40	24	1.24 ± 0.05	0.97 ± 0.09	0.83 ± 0.21
2.50	24	1.36 ± 0.06	1.03 ± 0.09	0.80 ± 0.23
2.50	25	1.36 ± 0.06	1.01 ± 0.11	0.84 ± 0.23
2.50	26	1.35 ± 0.06	0.98 ± 0.10	0.88 ± 0.23
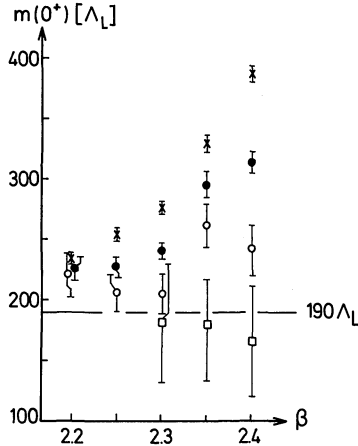
Fig. II.3. Scaling for the 0^+ mass gap, obtained from $m(1)$ (⊥), $m(2)$ (●), $\hat{m}(2)$ (⊘), and $m(3, 2)$ (⊡)

(after $\langle \mathbf{p}^2 \rangle$ subtraction) with our $\mathbf{p} = 0$ zero results from the best operator of length ≤ 8. We do not take into account our length 10 operators, or $t = 3$ results, in order to work in a similar approximation as the authors of [13, 14]. In this approximation we see no scaling beyond $\beta = 2.3$. We, therefore, attribute their result of [13, 14] to be due to the subtraction of the unknown $\langle \mathbf{p}^2 \rangle$.

With our high statistics we obtain also signals at distance $t = 3$. For the three best operators these results are collected in Table II.4. In Fig. II.3 we exhibit at each β-value distance $t = 1, 2, 3$ results for the best operator. Our results at distance $t = 3$ extend the scaling window up to $\beta = 2.4$. A conventional continuum limit estimate is

$$m(0^+) = (190 \pm 30) \Lambda_L^{SA}. \tag{II.6}$$

Table II.5. Critical length for a deconfinement temperature $T_c = 43 \Lambda_L$

β	T_c	$L_{\mathrm{crit}} = 1/T_c$
2.1	0.42	2.4
2.2	0.33	3.1
2.3	0.25	3.9
2.4	0.20	5.1
2.5	0.15	6.5

Table II.6. $m(2^+)$ MC results from the best operator and $m(2^+)$ SC results [26, 27] (last two orders)

β	OP	$m(1)$	$m(2)$	$\hat{m}(2)$	$SC, O(u^6)$	$SC, O(u^8)$
2.20	7	3.18 ± 0.04	$3.29 \pm^{\infty}_{0.45}$	$3.40 \pm^{\infty}_{0.93}$	3.42	3.17
2.25	7	3.04 ± 0.04	$2.72 \pm^{0.23}_{0.16}$	$2.40 \pm^{0.51}_{0.35}$	3.37	3.09
2.30	7	3.03 ± 0.04	$3.09 \pm^{0.58}_{0.26}$	$3.15 \pm^{1.19}_{0.55}$	3.33	3.01
2.35	24	2.89 ± 0.04	$2.54 \pm^{0.32}_{0.20}$	$2.18 \pm^{0.69}_{0.43}$	3.30	2.93
2.40	24	2.78 ± 0.03	2.38 ± 0.10	$1.97 \pm^{0.25}_{0.20}$	3.26	2.86
2.50	24	2.73 ± 0.04	$2.74 \pm^{0.30}_{0.19}$	$2.75 \pm^{0.62}_{0.40}$	3.20	2.70

This is slightly higher than the previous result $m(0^+) = (170 \pm 30) \Lambda_L^{\mathrm{SA}}$ [8], obtained on an $4^3 \cdot 16$ lattice. Even more notable finite size effects are found by comparing correlations for identical operators on the $4^3 \cdot 16$ and the 8^4 lattice, even at distance $t = 1$ clear discrepancies exist. This is argued to be due to the finite temperature-like phase transition for the small spacelike part of the $4^3 \cdot 16$ lattice. Indeed the estimate $T_c = 43 \Lambda_L^{\mathrm{SA}}$ [26] would give critical length scales as given in Table II.5.

The experience from string tension measurements shows, however, that more accurate data at distance $t \geq 3$ would be very desirable. There is some hope to achieve such results by using source methods (linear response together with the Langevin equation [27], study of boundary effects [28] or a "cold wall" method [29]).

II.3. Excited States

We have considered the excited spin states 0^-, 2^+, and 1^+. The irreducible representations of the cubic group on the Wilson loops up to length 8 are classified in [11]. According to this classification we have constructed the $A_1^-(0^-)$, $E^+(2^+)$ and $T_1^+(1^+)$ representations, whenever possible for a given Wilson loop.

In contrary to [14] our lowest excited state is the 2^+ tensor. For this state our results from the best operators are collected in Table II.6. As before in Sect. II.1 the best operator is defined to be the one which gives lowest mass values at distance $t = 1$. The $m(2, 0)$ and $m(2, 1)$ values are, of course, better upper bounds than the $m(1, 0)$ values. Within the large statistical noise it is, however, not possible to give a

Table II.7. Mass ratios $m(2^+)/m(0^+)$

β	$m(1)$	$m(2)$	$\hat{m}(2)$
2.20	1.79	1.90	2.02
2.25	1.81	1.77	1.71
2.30	1.86	2.19	2.63
2.35	1.68	1.65	1.60
2.40	1.56	1.65	1.77

Table II.8. Best results for 0^- and mass ratios $0^-/0^+$

β	OP	$m(1)$	$0^-/0^+$ $(t=1)$
2.20	21	$4.42 \pm^{0.21}_{0.17}$	2.48
2.25	8	$4.44 \pm^{0.14}_{0.13}$	2.64
2.30	8	$4.16 \pm^{0.19}_{0.16}$	2.55
2.35	8	$4.08 \pm^{0.39}_{0.28}$	2.37
2.40	8	$3.88 \pm^{0.11}_{0.10}$	2.18

Table II.9. Best results for 1^+ and mass ratios $1^+/0^+$

β	OP	$m(1)$	$1^+/0^+$ $(t=1)$
2.20	13	$5.04 \pm^{0.22}_{0.18}$	2.83
2.25	10	$5.03 \pm^{0.19}_{0.15}$	3.05
2.30	8	5.00 ± 0.13	3.07
2.35	21	$4.82 \pm^{0.21}_{0.17}$	2.80
2.40	21	$4.83 \pm^{0.22}_{0.19}$	2.71

reliable estimate of the expected lowering. Comparing the distance $t=2$ results for $\beta = 2.25$, 2.30 and $\beta = 2.35$ we find that even with our high statistics we do not obtain reliable error bars for these results. See Sect. III.3 for a related more detailed discussion.

In Table II.6 we have also given the two last orders from the strong coupling (SC) expansion [30, 31] in the character variable u. There is amazingly good agreement between the SC u^8 and the MC $m(1)$ results, indicating that the E^+ SC series may – in contrast to the A_1^+ SC series – still be convergent in the considered β-region or at least in part of it. As the cubic symmetry is an exact symmetry of the lattice such a possibility exists. For the convenience of the reader we collect in Table II.7 mass ratios $m(2^+)/m(0^+)$ as obtained by dividing the best 2^+ and 0^+ results. If we optimistically *assume* that the 2^+ state likes to scale for $\beta \geq 2.2$ we would obtain the order of magnitude

$$m(2^+) \approx 1.8\, m(0^+) \tag{II.7}$$

Table II.10. Considered momentum eigenstates

n_i^1	n_i^2	n_i^3	i
0	0	0	1
1	0	0	2
0	1	0	3
0	0	1	4
1	1	0	5
1	0	1	6
0	1	1	7
1	-1	0	8
1	0	-1	9
0	1	-1	10
1	1	1	11
2	0	0	12
0	2	0	13
0	0	2	14

from analyzing Table II.7. We have to emphasize that the low $m(1)$-ratios for $\beta \geq 2.35$ are meaningless, because at these values the mass estimates for 0^+ at distance $t = 1$ are already in the spin wave region [8]. The order of magnitude (II.7) is consistent with MC data of previous investigations [14] and also with results [32] as obtained using Manton's action.

Finally, Table II.8 contains our best 0^- and the Table II.9 our best 1^+ results. Only $m(1)$ values are given, because results at distance $t = 2$ are statistical noise. We also give the corresponding $0^-/0^+$ and $1^+/0^+$ mass ratios. Taking into account β-values up to $\beta = 2.30$ we find the orders of magnitude

$$m(0^-) \approx 2.5 \, m(0^+), \tag{II.8}$$

$$m(1^+) \approx 3 \, m(0^+). \tag{II.9}$$

Even more than for the 2^+ state, it is obscure whether these numbers have any meaning for the continuum limit $a(\beta) \to 0$.

II.4. Energy-Momentum Dispersion

In this section we consider momentum states for the $A_1^+(0^+)$ and the $E^+(2^+)$ states. In case of the A_1^+ representation we construct momentum eigenstates for all Wilson loops up to length 6, whereas for the E^+ representation we only take the 1-plaquette operator. In each case our momenta are $\mathbf{K}_i = \dfrac{\mathbf{n}_i}{2\pi L}$ $(L = 8)$, with $\mathbf{n}_i = (n_i^1, n_i^2, n_i^3)$, and $i = 1, \ldots, 14$ as given in Table II.10. As in [33] we construct the considered irreducible representations of the cubic group on appropriate spacelike cubes $C_j(\mathbf{x}, t)$, and perform the Fourier transform for these cube operators.

$$\tilde{C}_j(\mathbf{K}, t) = \sum_{\mathbf{x}} e^{i\mathbf{K}\mathbf{x}} C_j(\mathbf{x}, t).$$
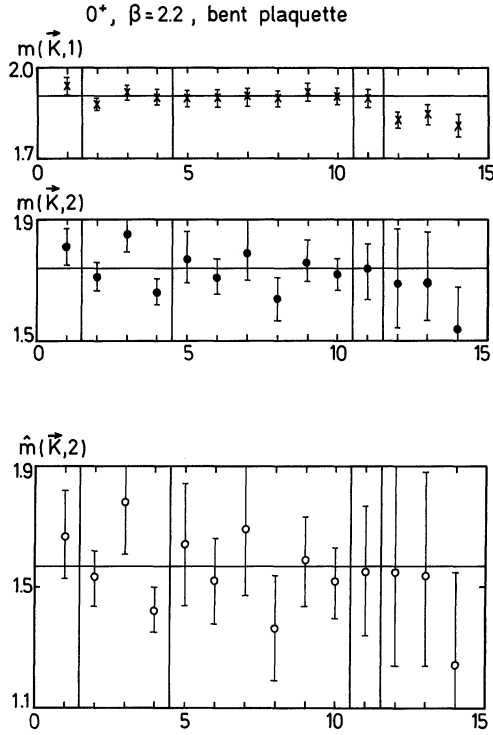
Fig. II.4. Results for 0^+ momentum states at $\beta = 2.2$

Different irreducible representations of the cubic group do not mix up to order $\mathbf{K}^2$. This means we obtain good projections on J^P eigenstates for small momenta and short distances. Otherwise, 0^+ will finally win.

Let us define

$$m(\mathbf{K}, t) = \sqrt{E(\mathbf{K}, t, 0)^2 - \mathbf{K}^2} \tag{II.10a}$$

and

$$\hat{m}(\mathbf{K}, t) = \sqrt{E(\mathbf{K}, t, 1)^2 - \mathbf{K}^2}, \tag{II.10b}$$

where $E(\mathbf{K}, t_2, t_1)$ is in analogy to Eq. (II.5) a finite distance definition of the energy of the momentum $\mathbf{K}$ state:

$$E(\mathbf{K}, t_2, t_1) = \frac{-1}{t_2 - t_1} \ln \left(\frac{\mathrm{Re} \, \overline{\langle \widetilde{C}_j(\mathbf{K}, t_2) \rangle} \widetilde{C}_j(\mathbf{K}, 0) \rangle}{\mathrm{Re} \, \langle \widetilde{C}_j(\mathbf{K}, t_1) \widetilde{C}_j(\mathbf{K}, 0) \rangle} \right) \quad (t_2 > t_1). \tag{II.11}$$

Using these definitions we find for the 0^+ state restoration of Lorentz invariance in the considered β-region ($\beta \geq 2.2$). This is illustrated in Fig. II.4. From the now considered operators the bent plaquette (operator #3 of Fig. I.1) is the best operator at $\beta = 2.2$. At distance $t = 2$ and already $t = 1$ we find restoration of Lorentz invariance for the 11 lowest momenta ($i = 1, ..., 11$ as defined in Table
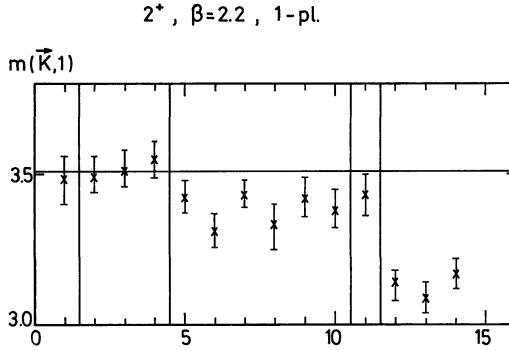
2^+ , $\beta = 2.2$, 1-pl.

Fig. II.5. Results for 2^+ momentum state at $\beta = 2.2$
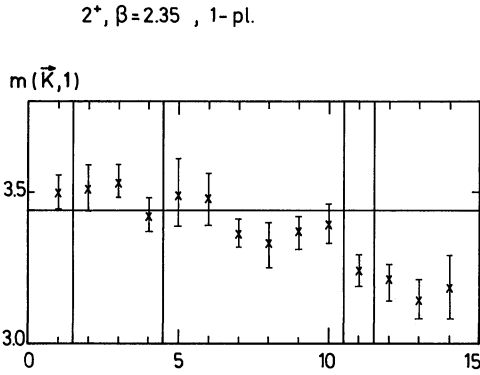
2^+, $\beta = 2.35$, 1-pl.

Fig. II.6. Results for 2^+ momentum states at $\beta = 2.35$

II.10). The horizontal line is the mean value calculated from these 11 momenta. The last three momenta deviate due to the finite lattice spacing. Indeed replacing

$$\mathbf{K}^2 \rightarrow \sum_{i=1}^{3} (2 - 2\cos K_i) \qquad (II.12)$$

gives also consistency with Lorentz invariance for these momenta. [For the first 10 momenta the change under the replacement (II.12) is numerically very small.]

In Fig. II.4 momenta within vertical lines have identical $\mathbf{K}^2$ and hence identical $E(\mathbf{K}, t_2, t_1)$.

For all β we find their energies to be statistically rather independent. Therefore, we may considerably increase the MC statistics by measuring momentum eigenstates for the low lying momenta and by using Lorentz invariance. In the present case we would win a factor $\lesssim 11$. Independently a similar observation has been made in [34].

For the 2^+ state the situation is depicted in Figs. II.5 and II.6. Only distance $t = 1$ correlations are sufficiently out of the statistical noise to allow clear conclusions. At $\beta = 2.2$ we find consistency with Lorentz invariance only for the first 4 momenta, whereas at $\beta = 2.35$ it is found for the first 10 momenta. The

Table III.1. Rectangular Wilson loops on the 8^4 lattice

β	1.5	1.6	1.7	1.8	1.9	2.0
W_{11}	0.5617	0.6003	0.6347	0.6629	0.6856	0.7043
	± 0.0002	± 0.0004	± 0.0003	± 0.0002	± 0.0002	± 0.0001
W_{12}	0.3118	0.3629	0.4114	0.4529	0.4866	0.5146
	± 0.0003	± 0.0007	± 0.0006	± 0.0003	± 0.0004	± 0.0002
W_{22}	0.1002	0.1437	0.1920	0.2381	0.2771	0.3101
	± 0.0003	± 0.0008	± 0.0009	± 0.0003	± 0.0007	± 0.0003
W_{13}	0.1744	0.2220	0.2707	0.3145	0.3512	0.3827
	± 0.0003	± 0.0007	± 0.0007	± 0.0003	± 0.0005	± 0.0002
W_{14}	0.0977	0.1362	0.1787	0.2193	0.2546	0.2853
	± 0.0002	± 0.0006	± 0.0007	± 0.0003	± 0.0006	± 0.0002
W_{23}	0.0337	0.0604	0.0959	0.1341	0.1688	0.1997
	± 0.0002	± 0.0005	± 0.0009	± 0.0003	± 0.0008	± 0.0003
W_{24}	0.0114	0.0258	0.0487	0.0769	0.1049	0.1310
	± 0.0001	± 0.0003	± 0.0008	± 0.0004	± 0.0008	± 0.0003
W_{33}	0.0070	0.0187	0.0390	0.0655	0.0929	0.1187
	± 0.0001	± 0.0003	± 0.0007	± 0.0004	± 0.0009	± 0.0003
W_{43}	0.0017	0.0060	0.0164	0.0333	0.0532	0.0732
	± 0.0001	± 0.0001	± 0.0005	± 0.0004	± 0.0008	± 0.0003
W_{44}	0.00012	0.0015	0.0059	0.0154	0.0289	0.0432
	± 0.00015	± 0.0001	± 0.0002	± 0.0005	± 0.0007	± 0.0007
β	1.45	1.55	1.65	1.75	1.85	1.95
$\beta^2 \partial_\beta W_{11}$	0.856	0.927	0.937	0.864	0.777	0.711
	± 0.006	± 0.013	± 0.014	± 0.013	± 0.011	± 0.012

horizontal lines are the mean values as calculated from the corresponding momentum eigenstates. As the momentum $K = 0$ 2^+ mass is rather high, we find only small changes under the replacement (II.12).

III. Symanzik Tree-Improved Action

We now report our MC results as obtained with the TIA. As before we use the icosaeder subgroup [24]. Our high statistics glueball calculations are done on a $5^3 \cdot 8$ lattice. Additionally, we calculate with a rather mode rate statistics the string tension from Creutz ratios on a 8^4 lattice.

III.1. The String Tension

At each β-value we have done first 200 sweeps without measurements for reaching equilibrium and then 2000 sweeps with measurements. For the relevant values $1.5 \leq \beta \leq 2.0$, our Wilson loop results are collected in Table III.1. Error bars are calculated with respect to 10 bins. Because of correlations between successive bins
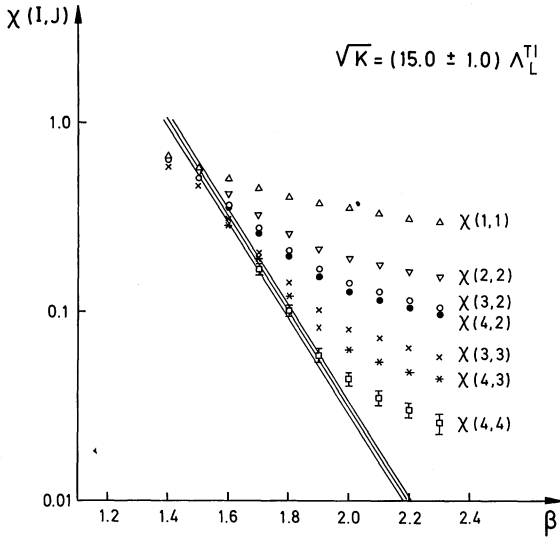
B. Berg, A. Billoire, S. Meyer, and C. Panagiotakopoulos

Fig. III.1. Conventional estimate of the string tension from Creutz ratios
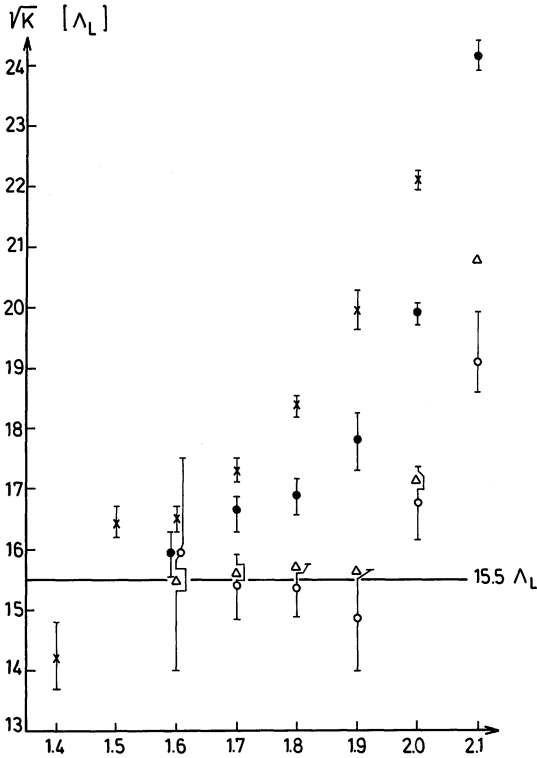
Fig. III.2. Relevant Creutz ratios on a precise physical scale: $\chi(3,3)$ $\not{\mathbb{X}}$, $\chi(4,3)$ ●, $\chi(4,4)$ $\bar{\underline{\circ}}$, and improved $\hat{\chi}(3,3)$ △

true error bars may be larger (see [11, 16] for a more detailed analysis). From W_{11} we can easily calculate the specific heat by numerical differentiation. For the convenience of the reader, we collect in Table III.1 also the specific heat as obtained from neighbour β-values. The peak is reached at $\beta \approx 1.65$.

Using Creutz ratios we give in Fig. III.1 a conventional plot for the scaling behaviour of the string tension. A scaling window is found and the continuum estimate is obtained from the envelope. The accuracy becomes much more obvious from Fig. III.2. These data in physical units of Λ_L^{TI} are plotted on a very precise scale. By a similar interpretation as in Sect. II.1 the $\chi(4, 4)$ results indicate the upper bound

$$\sqrt{K} \approx 15.5 \, \Lambda_L^{TI}. \tag{III.1}$$

This is lower than the previous results $\sqrt{K} \approx 17.9 \Lambda_L^{TI}$ [22] and $\sqrt{K} \approx 16.4 \Lambda_L^{TI}$ [23]. On the other hand, the potential analysis of [17] finds again (asymptotic) scaling deviations and a considerably lower value

$$\sqrt{K} \approx 12.5 \, \Lambda_L^{TI}. \tag{III.2}$$

Perturbative calculations [6, 35] of the Λ-ratio give

$$r = \Lambda_L^{TI}/\Lambda_L^{SA} = 4.13. \tag{III.3}$$

It is amazing to note that our results for $\sqrt{K^{TI}}/\sqrt{K^{SA}}$ and those of [17] are both consistent with the asymptotic estimate of Eq. (III.3).

A consistent string tension measurement using the improved action should involve improved loop operators. To the tree level order, improved Creutz ratios are given by [6]

$$\hat{\chi}(I, J) = \sum_{m, n} C_{mn} \ln [W(I + m, J + n)]. \tag{III.4}$$

Here $C_{mn} = C_{nm}$ and the non-zero C_{mn} are listed in the following:

$$c_{11} = y + \tfrac{1}{3}, \quad c_{00} = 3y + \tfrac{5}{4}, \quad c_{-1-1} = 1 - 3y, \tag{III.5a}$$

$$c_{-2-2} = -y - \tfrac{1}{12}, \quad c_{10} = -2y - \tfrac{1}{3}, \quad c_{-1-2} = 2y, \tag{III.5b}$$

$$c_{1-1} = y, \quad c_{0-2} = -y + \tfrac{1}{12}, \quad c_{0-1} = -1. \tag{III.5c}$$

y is a free parameter. (Note that the standard Creutz ratios are obtained with $c_{00} = 1$, $c_{0-1} = -1$, $c_{-1-1} = -1$, and all other $c_{mn} = 0$.)

We tried three choices:

$$\text{(a) } y = -\tfrac{1}{2}, \quad \text{(b) } y = 0, \quad \text{(c) } y = -\tfrac{1}{3}. \tag{III.6}$$

(a) and (b) are close to the standard Creutz ratios and (c) avoids W_{44}, which is the noisiest Wilson loop. Together with $\chi(3, 3)$ and $\chi(4, 4)$ we collect the results for $\hat{\chi}(3, 3)(a, b, c)$ in Table III.2.

There is y-independence up to an excellent precision and the $\hat{\chi}(3, 3)$ values are well compatible with $\chi(4, 4)$. This shows that the *improvement works* in a consistent way. In Fig. III.2 the triangles are mean values from our three considered $\hat{\chi}(3, 3)$ definitions, and there is good consistency with asymptotic scaling.

Table III.2. $\chi(3,3)$, $\chi(4,4)$, and improved string tensions $\hat{\chi}(3,3)$

β	1.6	1.7	1.8	1.9	2.0	2.1
$\chi(3,3)$	0.3052	0.2058	0.1416	0.1020	0.0799	0.0726
$\chi(4,4)$	0.2837	0.1625	0.0987	0.0566	0.0440	0.0346
$\chi(3,3)$(a)	0.2669	0.1670	0.1043	0.0634	0.0468	0.0414
$\chi(3,3)$(b)	0.2689	0.1671	0.1054	0.0640	0.0480	0.0420
$\chi(3,3)$(c)	0.2607	0.1666	0.1010	0.0613	0.0429	0.0398

Table III.3. Rectangular spacelike Wilson loops on a $5^3 \cdot 8$ lattice

β	W_{11}	W_{12}	W_{22}	Sweeps
1.45	0.5412 ±0.0001	0.2864 ±0.0002	0.0818 ±0.0002	40,000
1.50	0.5613 ±0.0001	0.3112 ±0.0002	0.0997 ±0.0902	40,000
1.55	0.58125 ±0.00008	0.3371 ±0.0002	0.1206 ±0.0002	122,000
1.60	0.6003 ±0.0002	0.3628 ±0.0002	0.1437 ±0.0003	80,000
1.65	0.61888 ±0.00008	0.3891 ±0.0002	0.1698 ±0.0002	164,000
1.70	0.63599 ±0.00008	0.4141 ±0.0002	0.1968 ±0.0002	160,000
1.75	0.6513 ±0.0002	0.4369 ±0.0003	0.2227 ±0.0004	42,000
1.80	0.6643 ±0.0002	0.4560 ±0.0003	0.2443 ±0.0004	40,000
1.90	0.68617 ±0.00004	0.48824 ±0.00006	0.2811 ±0.0001	160,000
2.00	0.70446 ±0.00007	0.5152 ±0.0002	0.3121 ±0.0003	40,000

III.2. The Mass Gap $m(0^+)$

Our glueball calculations are carried out on a $5^3 \cdot 8$ lattice. In view of the double plaquette involved in the Symanzik TIA a $5^3 \cdot 8$ lattice seems to be the smallest feasible lattice. As in [11, 20] our MC calculation is based on 21 Wilson loops W_i ($i = 1, ..., 21$) of length ≤ 8. We only measure spacelike Wilson loops. In Table III.3 we give mean values for the considered rectangular loops. As is obvious from this table we have collected a very high statistics of up to 160,000 sweeps at some β-values. This was mainly done for hunting the 2^+ state (see next section). We have done first 1200 sweeps for thermalization and carried out measurements after every second sweep.
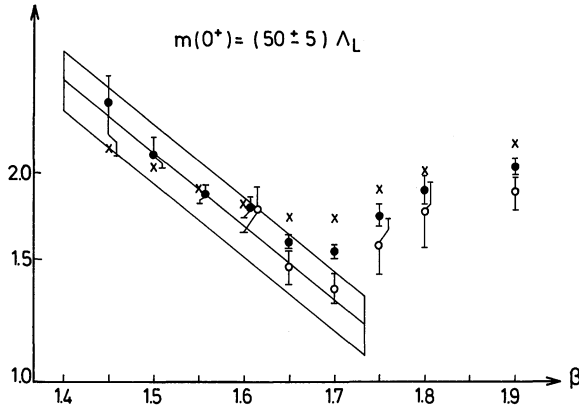
Fig. III.3. Scaling for the 0^+ mass gap

Finite distance glueball masses and best operators are defined as in Sect. II.2. We only consider correlations up to distance $t=2$. In Table III.4 we have for the three best operators collected the mass results. These three operators give always nearly identical numerical values. As depicted in Fig. III.3 we find a window $1.45 \leq \beta \leq 1.70$, where our distance $t=2$ data are in agreement with asymptotic scaling. The data of Fig. III.3 are always taken from the best operator of Table III.4.

As discussed in the introduction, the MCV method is in trouble[3] in the case of the improved action. This may be illustrated by the lowest order SC expansion for connected plaquette-plaquette correlations in the A_1^+ representation of the cubic group. Up to a positive proportionality constant one obtains[4] the following leading behaviour:

$$\langle \Box(0)\,\Box(t)\rangle_c = \begin{cases} (\tfrac{5}{3}\beta/4)^4 & (t=1) \\ (-\tfrac{1}{12}\beta/4)^4 & (t=2) \\ (\tfrac{5}{3}\beta/4)^4(-\tfrac{1}{12}\beta/4)^4 & (t=3) \\ (-\tfrac{1}{12}\beta/4)^8 & (t=4) \end{cases} \qquad (\text{III.7})$$

and $\langle \Box(0)\,\Box(t)\rangle_c = \text{const}$,

$$\begin{cases} (c_1\beta)^2(c_2\beta)^2(c_2\beta)^{2K}(c_1\beta)^2\,, & t=2K+1\,, & K\geq 2\,, \\ (c_1\beta)^2(c_2\beta)^2(c_2\beta)^{2K-1}(c_1\beta)^2\,, & t=2K\,, & K\geq 3\,, \end{cases}$$

with $c_1 = \tfrac{5}{3}$, $c_2 = -\tfrac{1}{12}$ (const >0).

For $t \to \infty$ we obtain from the *absolute value* of the correlation the leading order glueball mass

$$m(0^+) = -\ln\beta\,. \qquad (\text{III.8})$$

---

3   In the case of Manton's action the negative eigenvalues of the transfer matrix are not a severe problem for a MCV calculation [32]
4   We would like to thank G. Münster for clarifying discussions on this subject

B. Berg, A. Billoire, S. Meyer, and C. Panagiotakopoulos

Table III.4. $m(0^+)$ results from the best three operators

β	OP	$m(1)$	$m(2)$	$\hat{m}(2)$
1.45	8	2.17 ± 0.03	$2.29 \pm^{0.25}_{0.17}$	$2.40 \pm^{0.53}_{0.36}$
1.45	10	2.19 ± 0.03	$2.26 \pm^{0.24}_{0.17}$	$2.33 \pm^{0.51}_{0.35}$
1.45	21	2.19 ± 0.03	$2.24 \pm^{0.20}_{0.14}$	$2.30 \pm^{0.41}_{0.31}$
1.50	6	2.07 ± 0.03	$2.15 \pm^{0.14}_{0.11}$	$2.23 \pm^{0.50}_{0.24}$
1.50	8	2.05 ± 0.03	$2.16 \pm^{0.13}_{0.09}$	$2.28 \pm^{0.26}_{0.22}$
1.50	21	2.03 ± 0.03	$2.12 \pm^{0.13}_{0.09}$	$2.22 \pm^{0.26}_{0.21}$
1.55	6	1.89 ± 0.02	1.86 ± 0.05	1.83 ± 0.11
1.55	13	1.89 ± 0.02	1.87 ± 0.05	1.85 ± 0.12
1.55	21	1.89 ± 0.02	1.87 ± 0.05	1.84 ± 0.12
1.60	6	1.80 ± 0.03	1.78 ± 0.06	1.77 ± 0.13
1.60	13	1.80 ± 0.03	1.78 ± 0.05	1.77 ± 0.13
1.60	21	1.82 ± 0.03	1.81 ± 0.06	1.81 ± 0.13
1.65	6	1.73 ± 0.02	1.59 ± 0.04	1.46 ± 0.08
1.65	13	1.72 ± 0.02	1.51 ± 0.03	1.46 ± 0.08
1.65	21	1.77 ± 0.02	1.64 ± 0.04	1.50 ± 0.09
1.70	6	1.73 ± 0.02	1.55 ± 0.03	1.38 ± 0.07
1.70	13	1.72 ± 0.01	1.54 ± 0.03	1.36 ± 0.06
1.70	21	1.79 ± 0.01	1.60 ± 0.03	1.41 ± 0.06
1.75	6	1.89 ± 0.04	1.74 ± 0.06	1.60 ± 0.14
1.75	7	1.94 ± 0.04	1.74 ± 0.06	1.54 ± 0.14
1.75	13	1.89 ± 0.04	1.73 ± 0.06	1.57 ± 0.14
1.80	6	2.03 ± 0.04	1.91 ± 0.09	$1.78 \pm^{0.21}_{0.18}$
1.80	7	2.08 ± 0.04	1.88 ± 0.07	$1.68 \pm^{0.19}_{0.16}$
1.80	13	2.01 ± 0.03	1.89 ± 0.09	$1.76 \pm^{0.21}_{0.18}$
1.90	6	2.22 ± 0.02	2.06 ± 0.05	1.91 ± 0.11
1.90	13	2.20 ± 0.02	2.04 ± 0.05	1.87 ± 0.10
1.90	21	2.29 ± 0.02	2.14 ± 0.06	1.99 ± 0.14
2.00	5	2.31 ± 0.04	$2.15 \pm^{0.14}_{0.11}$	$2.00 \pm^{0.31}_{0.25}$
2.00	6	2.34 ± 0.04	$2.11 \pm^{0.12}_{0.09}$	$1.89 \pm^{0.16}_{0.12}$
2.00	13	2.32 ± 0.04	2.12 ± 0.12	$1.91 \pm^{0.28}_{0.23}$

At small distances t the fall-off of the correlation function is, however, rather different.

As TIA and SA are in the same universality class, one expects the problem to be less important in the continuum limit $\beta \to \infty$. In our β-region we find for all considered operators positive correlations at distance $t = 1, 2$. At our low β-values ($\beta = 1.45, 1.55$) $m(2, 0)$ results are systematically higher than $m(1, 0)$ results. Because of the interaction range going over two lattice spacings, one should discard the $m(1, 0)$ results for the purpose of estimating the mass gap. Our selection of best operators is based on distance $t = 1$ correlations, and one may now doubt this procedure. But our high MC statistics allow us also to select directly the lowest $m(2, 0)$ result. With only one exception ($\beta = 1.75$) we obtain always one of our three best operators (Table III.4), and at $\beta = 1.75$ the result we find remains within

Table III.5. $m(2^+)$ results for the best two operators

β	OP	$m(1)$	$m(2)$	$\hat{m}(2)$
1.45	2	3.35 ± 0.06	$4.55 \pm_{1.44}^{\infty}$	$5.75 \pm_{2.34}^{\infty}$
1.45	7	3.34 ± 0.04	∞	∞
1.50	7	3.18 ± 0.06	$3.19 \pm_{0.42}^{\infty}$	$3.20 \pm_{0.88}^{\infty}$
1.50	8	3.16 ± 0.04	∞	∞
1.55	7	3.12 ± 0.03	$3.14 \pm_{0.23}^{0.42}$	$3.15 \pm_{0.47}^{0.87}$
1.55	8	3.15 ± 0.03	$3.49 \pm_{0.33}^{1.26}$	$3.83 \pm_{1.68}^{2.54}$
1.60	7	2.94 ± 0.03	$2.84 \pm_{0.14}^{0.20}$	$2.73 \pm_{0.30}^{0.42}$
1.60	8	3.00 ± 0.03	$2.95 \pm_{0.21}^{0.35}$	$2.90 \pm_{0.44}^{0.72}$
1.65	7	2.93 ± 0.03	$2.93 \pm_{0.16}^{0.24}$	$2.93 \pm_{0.34}^{0.50}$
1.65	8	2.98 ± 0.01	$3.13 \pm_{0.21}^{0.38}$	$3.28 \pm_{0.44}^{0.78}$
1.70	5	2.93 ± 0.03	$2.61 \pm_{0.10}^{0.13}$	$2.29 \pm_{0.23}^{0.27}$
1.70	7	2.89 ± 0.03	$2.72 \pm_{0.12}^{0.16}$	$2.55 \pm_{0.27}^{0.34}$
1.75	5	2.90 ± 0.04	$2.68 \pm_{0.17}^{0.25}$	$2.46 \pm_{0.37}^{0.54}$
1.75	7	2.86 ± 0.04	$2.92 \pm_{0.24}^{0.47}$	$2.99 \pm_{0.52}^{0.97}$
1.80	5	2.94 ± 0.04	$2.75 \pm_{0.19}^{0.31}$	$2.57 \pm_{0.42}^{0.65}$
1.80	7	2.91 ± 0.04	$2.78 \pm_{0.21}^{0.37}$	$2.65 \pm_{0.45}^{0.77}$
1.90	5	2.81 ± 0.02	2.60 ± 0.09	2.39 ± 0.18
1.90	7	2.82 ± 0.02	2.72 ± 0.10	$2.61 \pm_{0.19}^{0.24}$
2.00	5	2.76 ± 0.03	$2.50 \pm_{0.10}^{0.13}$	$2.25 \pm_{0.23}^{0.28}$
2.00	7	2.81 ± 0.03	$2.57 \pm_{0.14}^{0.18}$	$2.32 \pm_{0.30}^{0.40}$

statistical errors unchanged. In summary, our procedure is consistent up to distance $t=2$. From Fig. III.3 our final estimate is

$$m(0^+) = (50 \pm 5)\, \Lambda_L^{TI}. \tag{III.9}$$

Comparing this with Eq. (II.6) gives us the Λ-ratio, $r_{mg} \approx 3.8$, in good agreement with universality.

III.3. Excited States

As for the SA we consider 0^-, 2^+, and 1^+ states. The warnings from Sect. III.2 with respect to the MCV method apply again. Within our practical restrictions we obtain results as presented in this section. Our lowest state is again the 2^+ tensor. For this state mass values from the best two operators at each β are collected in Table III.5, and results obtained from the best operators are also graphically depicted in Fig. III.4. There is no signal for asymptotic scaling, hence also no signal for scaling of the mass ratio $m(2^+)/m(0^+)$. Up to $\beta = 1.8$ distance $t=2$ results are (within their errors) even well compatible with the $t=1$ results. After drastically increasing the MC statistics our previous [20] indication of asymptotic scaling in this β-region (from $t=2$ correlations) disappeared.

We illustrate this by drawing "continuum estimate" lines into Fig. III.4, which are very different from those of [20]. This demonstrates the arbitrariness, but does
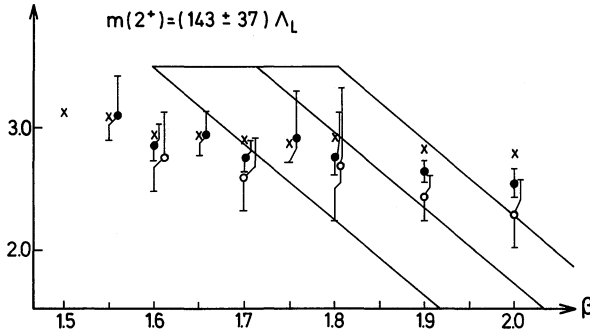
Fig. III.4. 2^+ state results

not rule out the previous estimate. In particular, it should be mentioned in this connection, that the finite temperature phase transition is around $\beta \approx 1.6$–1.7 (see also [17]).

Results of [20] are based on 40,000 sweeps at each β-value. We added new β-values and increased the statistics up to 160,000 sweeps at some selected β-values. Independently of the total number of sweeps we calculate at each β error bars by dividing our complete set of data into 20 bins. Even in the range 40,000–160,000 sweeps the $m(2)$ and $\hat{m}(2)$ error bars do not obey the asymptotic $1/\sqrt{N_{\text{sweeps}}}$ behaviour. This indicates the existence of correlations in computer time over an enormous number of sweeps and/or very rare but important events.

For the convenience of the reader we collect in Table III.6 mass ratios $m(2^+)/m(0^+)$ as obtained by dividing the best 2^+ and 0^+ results. $m(1)$ ratios are of particular interest because of their statistical reliability. The reached maximum is lower than in the case of the SA. (See the corresponding Table II.7.) Also the maximum is reached at a much smaller correlation length, because the $m(0^+)$ scaling window is shifted to a smaller correlation length as compared with the SA. The correlation length $1/m(0^+)$ as obtained from our mass gap estimates (II.6) and (II.9) is given in Table III.7 for the relevant β-values of both actions. Assuming that

Table III.6. Mass ratios $m(2^+)/m(0^+)$

β	$m(1)$	$m(2)$	$\hat{m}(2)$
1.45	1.54	∞	∞
1.50	1.56	∞	∞
1.55	1.65	1.69	1.72
1.60	1.63	1.60	1.54
1.65	1.70	1.84	2.01
1.70	1.68	1.77	1.88
1.75	1.51	1.69	1.90
1.80	1.45	1.47	1.51
1.90	1.28	1.27	1.28
2.00	1.19	1.16	1.13

Table III.7. Correlation for SA and TIA

SA		TIA	
β	ξ	β	ξ
2.20	0.69	1.55	0.53
2.25	0.79	1.60	0.60
2.30	0.89	1.65	0.68
2.35	1.01	1.70	0.76
2.40	1.14	1.75	0.86

Table III.8. $m(0^-)$ results from the best operator

β	OP	$m(1)$	$0^-/0^+$ $(t=1)$
1.45	21	$4.78 \pm^{0.23}_{0.19}$	2.20
1.50	21	$4.32 \pm^{0.25}_{0.20}$	2.13
1.55	6	4.21 ± 0.13	2.23
1.60	21	4.12 ± 0.11	2.29
1.65	6	3.91 ± 0.06	2.27
1.70	21	3.93 ± 0.06	2.28
1.75	6	3.78 ± 0.13	2.00
1.80	6	3.45 ± 0.12	2.34
1.90	21	3.60 ± 0.05	2.06
2.00	21	3.59 ± 0.08	1.88

Table III.9. $m(1^+)$ results from the best operator

β	OP	$m(1^+)$	$1^+/0^+$ $(t=1)$
1.45	11	$5.53 \pm^{0.43}_{0.30}$	2.54
1.50	19	$5.17 \pm^{0.30}_{0.23}$	2.55
1.55	13	5.07 ± 0.14	2.68
1.60	21	4.91 ± 0.12	2.73
1.65	13	4.92 ± 0.11	2.86
1.70	13	4.76 ± 0.08	2.77
1.75	19	4.46 ± 0.15	2.36
1.80	21	4.70 ± 0.15	2.34
1.90	8	4.54 ± 0.09	2.06
2.00	9	4.36 ± 0.12	1.89

the rather smooth behaviour of $m(1)$ ratios up to the maximum at $\xi \approx 0.68$ gives an indication about the continuum limit behaviour, we would obtain for the TIA

$$m(2^+) \approx 1.6 \, m(0^+) \qquad (\text{III.10})$$

as compared with $m(2^+) \approx 1.8 \, m(0^+)$ in case of the SA.

In Tables III.8 and III.9 we give our $m(1)$ results from the best operators for 0^- and 1^+ states. For these states distance $t = 2$ results are noise. We also give the mass ratios $0^-/0^+$ and $1^+/0^+$. By taking into account ratios up to the maximum at $\beta = 1.65$, we find the order of magnitude

$$m(0^-) \approx 2.2 \, m(0^+), \qquad (\text{III.11})$$

$$m(1^+) \approx 2.8 \, m(0^+). \qquad (\text{III.12})$$

As for the 2^+ state these ratios are somewhat lower than the corresponding ratios (II.8) and (II.9) in case of the SA.

III.4. Energy-Momentum Dispersion

In this section we consider momentum eigenstates for the $A_1^+(0^+)$ and the $E^+(2^+)$ states. Details, in particular the considered operators, are as described for the SA in
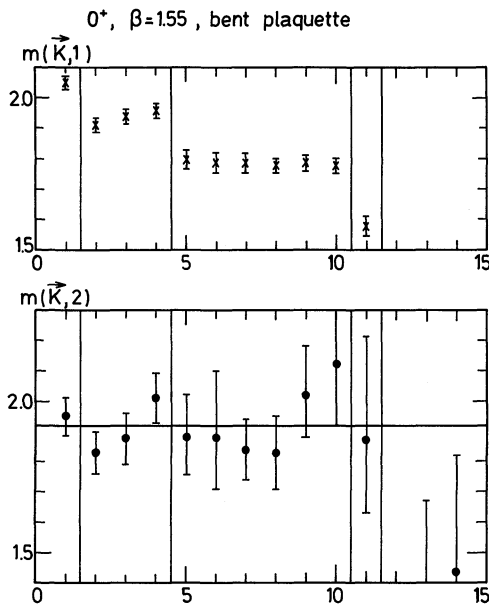
Fig. III.5. Results for 0^+ momentum eigenstates. (Equation II.12 is used for $\mathbf{K}^2$)

Sect. II.4. For $i = 1, \ldots, 14$ the momenta are defined in Table II.10. Of course, we have now $L = 5$ and the MC statistics of Table III.3.

As compared with the SA the energy-momentum dispersion is *not* improved. Typical results for the 0^+ state are depicted in Fig. III.5. As $L = 5$ is rather small, we always replace $\mathbf{K}^2$ by means of Eq. (II.12) for the figures of this section. For all considered higher momenta the relativistic energy-momentum dispersion is clearly violated at distance $t = 1$. This has to be seen in contrast to the corresponding SA results of Fig. II.4. We attribute the bad behaviour of the TIA to the already discussed problems with the transfer matrix, implying strong reservations against all distance $t = 1$ results. At distance $t = 2$ we find restoration of Lorentz invariance within the statistical errors.

The 2^+ state results, as for a typical example depicted in Fig. III.6, look similar. At distance $t = 2, 2^+$ data are, however, so noisy that no clear conclusions are possible. The lack of Lorentz invariance at distance $t = 1$ is particularly ugly, if one thinks about using higher momentum eigenstates for improving the 2^+ state MC statistics at distance $t = 2$. In contrast to the SA no self-consistent procedure would be possible. For both actions calculations of the 2^+ state using momentum states may suffer from the 0^+ mixing.

IV. Summary and Conclusions

Within the limits of our approximations we obtain the following results: $\sqrt{K} \approx 69 \, \Lambda_L^{SA}$ (II.3), $m(0^+) \approx 190 \, \Lambda_L^{SA}$ (II.6) for the SA and $\sqrt{K} \approx 15.5 \, \Lambda_L^{TI}$ (III.1),
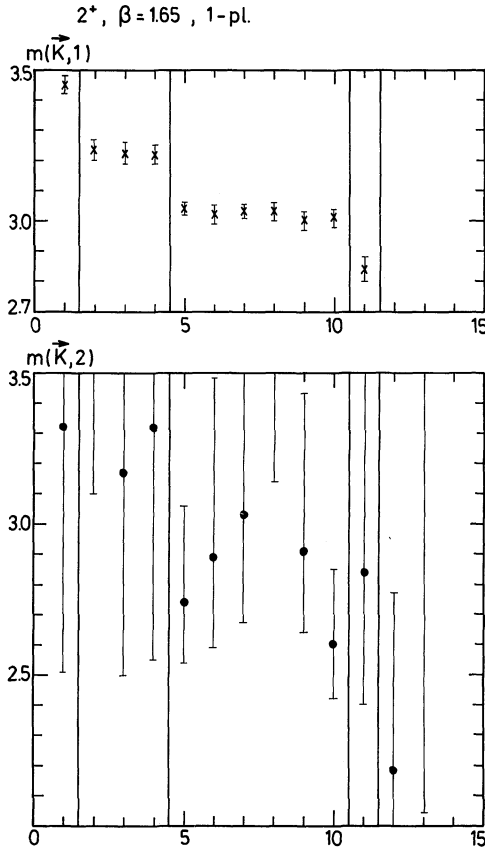
Fig. III.6. Results for 2^+ momentum eigenstates. (Equation II.12 is used for $\mathbf{K}^2$)

$m(0^+) \approx 50 \, \Lambda_L^{\mathrm{TI}}$ (III.9) for the TIA. This gives for the Λ-ratio $r = \Lambda_L^{\mathrm{TI}}/\Lambda_L^{\mathrm{SA}} = 4.13$ [6, 35] the MC estimates $r_{\sqrt{K}} \approx 4.5$ and $r_{m(0^+)} \approx 3.8$ in consistency with universality.

Results for the excited states $2^+, 0^-, 1^+$, due to lack of clear scaling signals, are rather inconclusive. Very tentative orders of magnitude are: $m(2^+) \approx 1.6$–$1.8 \, m(0^+)$, $m(0^-) \approx 2.2$–$2.5 \, m(0^+)$, and $m(1^+) \approx 2.8$–$3.0 \, m(0^+)$. The lower values corresponds always to the TIA and the higher value to the SA.

Finally, we have calculated energies for momentum eigenstates. In case of the 0^+ state we find the relativistic energy-momentum dispersion restored for both actions. The SA behaves nicer than the TIA, as the restoration of Lorentz invariance already happens at distance $t = 1$. This allows us to establish such a result also for the 2^+ state.

A future MCV calculation of the glueball spectrum should be based on important operators only, and use – at least for the lowest state – restoration of Lorentz invariance for improving the MC statistics. For the different actions and states the important ("best" at some values of β in the notation of Sects. II and III),

Table IV.1. Important operators

SA, 0^+:	6,			13,	21, 24.
SA, 2^+:	7,				21, 24.
SA, 0^-:	8,				21.
SA, 1^+:	8,	10,		13,	21.
TIA, 0^+:	5, 6, 7, 8,	10,		13,	21.
TIA, 2^+:	2, 5, 7, 8,				
TIA, 0^-:	6,				21.
TIA, 1^+:	8, 9,		11,	13,	19, 21.

Table IV.2. Size of scaling windows

	β_1	β_2	ξ_1	ξ_2	ξ_2/ξ_1
$\sqrt{K}$, SA	2.20^a	2.50^a	0.69	1.47	2.1
$m(0^+)$, SA	2.00^b	$2.4\,[2.25^b]$	0.42	$1.14\,[0.78]$	$2.7\,[1.9]$
$\sqrt{K}$, TIA	1.5	1.9	0.47	1.24	2.6
$m(0^+)$, TIA	1.45	1.7	0.42	0.76	1.8

[a] Incorporates also results of [16]
[b] Relies on [8], where a $4^3 \cdot 16$ lattice was used

operators are collected in Table IV.1. (The numbers are defined by means of Fig. I.1.) Doing a more detailed analysis, particularly emphasizing the 0^+ and 2^+ states, we find in conclusion everything well covered by measuring only correlations of the operators 6, 7, 13, 21, and 24.

The crucial question is, of course: does the improvement work? In Table IV.2 we collect approximate estimates for the beginning and end of the scaling windows obtained so far. Scaling (with reservations coming from [17]) of the TIA string tension sets on at a smaller correlation length than for the SA. Otherwise, scaling windows, if compared on similar lattices, look similar. Therefore, from a practical point of view, the improvement is modest. An important consistency check is, of course, the observation that the improved definitions [6] of Creutz ratios work well (see Sect. III.1).

For spectrum calculations the SA has the decisive advantage of a positive definite transfer matrix. Together with the greater computational simplicity, this is an important feature in favour of the SA.

Note added. After finishing the manuscript we became aware of an extension [36] of the work of [22].

References

1. Symanzik, K.: In: Mathematical problems in theoretical physics. Schrader et al. (eds.). Lecture Notes in Physics, Vol. 153. Berlin, Heidelberg, New York: Springer 1982
2. Symanzik, K.: Continuum limit and improved action in lattice theories. I. Principles and ϕ^4 theory. Nucl. Phys. B **226**, 187 (1983)
3. Berg, B., Meyer, S., Montvay, I., Symanzik, K.: Improved continuum limit in the lattice $O(3)$ non-linear sigma model. Phys. Lett. **126** B, 467 (1983)
   Falcioni, M., Martinelli, G., Paciello, M.L., Taglienti, B., Parisi, G.: A Monte Carlo simulation with an "improved" action for the $O(3)$ non-linear sigma model. Nucl. Phys. B **225**, (FS9), 313 (1983)
   For recent reviews see: Berg, B.: Preprint, DESY 83-120, published in the proceedings of the "International Symposium on the Theory of Elementary Particles," Ahrenshoop (DDR), 1983
   Meyer, S.: Talk presented at the Santa Barbara Workshop, 20.6.–1.7.83
4. Curci, G., Menotti, P., Paffuti, G.P.: Symanzik's improved lagrangian for lattice gauge theory. Phys. Lett. **130** B, 205 (1983)
5. Weisz, W.: Continuum limit improved lattice action for pure Yang-Mills theory. I. Nucl. Phys. B **212**, 1 (1983)
6. Weisz, P., Wohlert, R.: Nucl. Phys. B **236**, 137 (1984)
7. Berg, B.: Cargèse lectures 1983
8. Berg, B., Billoire, A., Rebbi, C.: Monte Carlo estimates of the $SU(2)$ mass gap. Ann. Phys. (NY) **142**, 185 (1982) and Addendum **146**, 470 (1983)
9. Falcioni, M., Marinari, E., Paciello, M.L., Parisi, G., Rapuano, F., Taglienti, B., Zhang, Yi-Chang: On the masses of the glueballs in pure $SU(2)$ lattice gauge theory. Phys. Lett. **110** B, 295 (1982)
10. Ishikawa, K., Schierholz, G., Teper, M.: The glueball mass spectrum in QCD: First results of a lattice Monte Carlo calculation. Phys. Lett. **110** B, 399 (1982)
11. Berg, B., Billoire, A.: Glueball spectroscopy in $4d SU(3)$ lattice gauge theory. I. Nucl. Phys. B **221**, 109 (1983) and: Glueball spectroscopy in $4d SU(3)$ lattice gauge theory. II. Nucl. Phys. B **226**, 405 (1983)
12. Berg, B., Meyer, S., Montvay, I.: Nucl. Phys. B **235** [FS11], 149 (1984)
13. Ishikawa, K., Schierholz, G., Teper, M.: Renormalization group behaviour of 0^+ and 2^+ glueball masses in $SU(2)$. Z. Phys. C **16**, 69 (1982)
14. Ishikawa, K., Schierholz, G., Teper, M.: Calculation of the glueball mass spectrum of $SU(2)$ and $SU(3)$ non-Abelian lattice gauge theories. I. Introduction and $SU(2)$. Z. Phys. C **19**, 327 (1983)
15. Creutz, M.: Asymptotic-freedom scales. Phys. Rev. Lett. **45**, 313 (1980)
16. Berg, B., Stehr, J.: $SU(2)$ lattice gauge theory and Monte Carlo calculations. Z. Phys. C **9**, 333 (1981)
17. Gutbrod, F., Montvay, I.: Phys. Lett. **136** B, 411 (1984)
18. Billoire, A., Marinari, E.: Phys. Lett. **139** B, 399 (1984)
19. Karsch, F., Lang, C.B.: Phys. Lett. **138** B, 176 (1984)
20. Berg, B., Billoire, A., Meyer, S., Panagiotakopoulos, C.: Monte Carlo calculation of $SU(2)$ glueball states with Symanzik's tree-level improved action. Phys. Lett. **133** B, 359 (1983)
21. Lüscher, M., Weisz, P.: On-shell improved lattice gauge theories. Commun. Math. Phys. **97**, 59–77 (1984)
22. Belforte, S., Curci, G., Menotti, P., Paffuti, G.P.: Monte Carlo calculations with Symanzik's improved action for QCD. Phys. Lett. **131** B, 423 (1983)
23. Fukugita, M., Kaneko, T., Niuya, T., Ukawa, A.: Measurement of the string tension in $SU(2)$ lattice gauge theory with action including six-link loops. Phys. Lett. **130** B, 73 (1983) and Addendum
24. Rebbi, C.: Phase structure of non-Abelian lattice gauge theories. Phys. Rev. D **21**, 3350 (1980)
    Petcher, D., Weingarten, D.: Monte Carlo calculations and a model of the phase structure for gauge theories on discrete subgroups of $SU(2)$. Phys. Rev. D **22**, 2465 (1980)
    Bhanot, G., Lang, C., Rebbi, C.: Comp. Phys. Commun. **25**, 275 (1982)

25. Stack, J.D.: Heavy quark potential in $SU(2)$ lattice gauge theory. Phys. Rev. D **27**, 412 (1983)
26. Engels, J., Karsch, F., Montvay, I., Satzs, H.: Finite size effects in euclidean lattice thermodynamics for non-interacting Bose and Fermi systems. Nucl. Phys. B **205** [FS5], 545 (1982)
27. Falcioni, M., Marinari, E., Paciello, M.L., Parisi, G., Taglienti, B., Zhang, Yi-Chang: Large-distance correlation functions for an $SU(2)$ lattice gauge theory. Nucl. Phys. B **215** [FS5], 265 (1983)
28. Mütter, K.H., Schilling, K.: Glueball mass from variant actions in lattice Monte Carlo simulations. Phys. Lett. **121** B, 267 (1983)
    Parisi, G.: Private communication
29. de Forcrand, Ph.: Work in progress
30. Münster, G.: Strong coupling expansions for the mass gap in lattice gauge theories. Nucl. Phys. B **190**, 439 (1981); Erratum B **205** [FS5], 545 (1982)
31. Seo, K.: Glueball mass estimate by strong coupling expansion in lattice gauge theories. Nucl. Phys. B **209**, 200 (1982)
32. Berg, B., Billoire, A., Koller,·K.: Monte Carlo calculation of $SU(2)$ glueball states with Manton's action. Nucl. Phys. B **233**, 50 (1984)
33. Kimura, N., Ukawa, A.: Energy-momentum dispersion of glueballs and the restoration of Lorentz invariance in lattice gauge theories. Nucl. Phys. B **205** [FS5], 637 (1982). See also: Berg, B., Panagiotakopolous, C.: Photon in $U(1)$ lattice gauge theory. Phys. Rev. Lett. **52**, 94 (1984)
34. Schierholz, G., Teper, M.: Phys. Lett. **136** B, 64, 69 (1984)
35. Bernreuther, W., Wetzel, W.: The relation between the Λ parameters of the standard and of the continuum limit improved lattice action for pure Yang-Mills theory. Phys. Lett. **132** B, 382 (1983)
    Iwasaki, Y., Sakai, S.: Phys. Lett. **136** B, 73 (1984)
36. Belforte, S., Curci, G., Menotti, P., Paffuti, G.: Phys. Lett. **137** B, 207 (1984)